

The H₂O₂ Stimulon in *Saccharomyces cerevisiae**

(Received for publication, January 30, 1998, and in revised form, June 12, 1998)

Christian Godon‡, Gilles Lagniel‡, Jaekwon Lee§, Jean-Marie Buhler‡, Sylvie Kieffer¶, Michel Perrot¶, Hélian Boucherie¶, Michel B. Toledano‡§, and Jean Labarre‡**

From the ‡Service de Biochimie et Génétique Moléculaire, CEA-Saclay, F-91191 Gif-sur-Yvette Cedex, France,

§Department of Pharmacology and Toxicology, College of Pharmacy, Rutgers University, Piscataway, New Jersey 08855,

¶Institut de Biochimie et de Génétique Cellulaires, UPR CNRS 9026, 33077 Bordeaux Cedex, France, and ¶Département de Biologie Moléculaire et Structurale, CEA-Grenoble, F-38054 Cedex 9, France

The changes in gene expression underlying the yeast adaptive stress response to H₂O₂ were analyzed by comparative two-dimensional gel electrophoresis of total cell proteins. The synthesis of at least 115 proteins is stimulated by H₂O₂, whereas 52 other proteins are repressed by this treatment. We have identified 71 of the stimulated and 44 of the repressed targets. The kinetics and dose-response parameters of the H₂O₂ genomic response were also analyzed. Identification of these proteins and their mapping into specific cellular processes give a distinct picture of the way in which yeast cells adapt to oxidative stress. As expected, H₂O₂-responsive targets include an important number of heat shock proteins and proteins with reactive oxygen intermediate scavenging activities. Exposure to H₂O₂ also results in a slowdown of protein biosynthetic processes and a stimulation of protein degradation pathways. Finally, the most remarkable result inferred from this study is the resetting of carbohydrate metabolism minutes after the exposure to H₂O₂. Carbohydrate fluxes are redirected to the regeneration of NADPH at the expense of glycolysis. This study represents the first genome-wide characterization of a H₂O₂-inducible stimulon in a eukaryote.

Aerobic organisms have to maintain a reduced cellular redox environment in the face of the prooxidative conditions characteristic of aerobic life. The incomplete reduction of oxygen to water during respiration leads to the formation of redox-active oxygen intermediates (ROI)¹ such as the superoxide anion radical (O₂⁻), hydrogen peroxide (H₂O₂), and the hydroxyl radical (OH[•]) (for review, see Refs. 1–3). ROI are also produced during the β-oxidation of fatty acids, and upon exposure to radiation, light, metals, and redox active drugs. Oxidative stress results from abnormally high levels of ROI which perturb the cell redox status and leads to damage to lipids, proteins, DNA, and eventually cell death. Living organisms constantly sense and adapt to such redox perturbations by the induction of batteries of genes or stimulons whose products act to maintain the cellular redox environment (4). In *Escherichia coli*, two distinct stimulons exist, one for H₂O₂ and the other for O₂⁻, each con-

sisting of a set of 30–40 proteins (for review, see Refs. 2, 5, and 6). The genes encoding nine of the H₂O₂-inducible proteins are controlled by the transcriptional regulator OxyR and include *katG* (catalase), *ahpCF* (an alkyl hydroperoxide reductase), *gorA* (glutathione reductase), and *dps* (a nonspecific DNA binding protein). The genes encoding nine of the O₂⁻-inducible proteins are controlled by the SoxR/S transcriptional regulators and include *sodA* (manganese superoxide dismutase), *zwf1* (glucose-6-phosphate dehydrogenase), *nfo* (DNA repair exonuclease IV), *fumC* (fumarase C), and *micF* (an antisense RNA regulator). Most of the remaining proteins of these stimulons are unknown, but their identification would increase our understanding of the mechanisms of cellular redox control and ROI metabolism. The yeast *Saccharomyces cerevisiae* can also adapt to both H₂O₂- and O₂⁻-generating drugs (7, 8) by the induction of two distinct but overlapping stimulons for H₂O₂ and O₂⁻ (9, 10). Yeast has the same defense mechanisms as higher eukaryotes (for review, see Refs. 11 and 12) and offers the power of genome-wide experimental approaches owing to the availability of the complete sequence of its genome. It therefore represents an ideal eukaryotic model in which to study the cellular redox control and ROI metabolism.

We recently established a general method to identify yeast proteins based on two-dimensional gel electrophoresis (13). We used this genome-wide experimental approach to characterize proteins whose expression is altered upon exposure to low doses of H₂O₂. Such an oxidative stress challenge results in a dramatic genomic response involving at least 167 proteins. Identification of these proteins and their mapping into cellular processes give a global view of the ubiquitous cellular changes elicited by H₂O₂ and provides the framework for understanding the mechanisms of cellular redox homeostasis and H₂O₂ metabolism.

MATERIALS AND METHODS

Strains and Growth Conditions—The yeast strain YPH98 (14) (*MATa ura3-52 lys2-801^{amber} ade2-101^{ochre} trp1-Δ1 leu2-Δ1*) was used for the analysis of the H₂O₂ response. The strain S288C (15) was used for protein spot identification. Strains were grown at 30 °C in a medium containing 0.67% yeast nitrogen base without amino acids (Difco), 2% glucose, buffered to pH 5.8 with 1% succinate and 0.6% NaOH. For YPH98, uracil, adenine, lysine, tryptophan and leucine (30 mg/liter) were added to the culture medium.

Identification of Protein Spots on Two-dimensional Gels—All the 32 new protein identifications were performed in the S288C strain background. Of these, three were identified by a peptide mass mapping approach using matrix-assisted laser desorption/ionization-time-of-flight/mass spectrometry (16). The remaining 29 were identified by the method described in Maillet *et al.* (13). This method is based on the determination of the amino acid composition of a given protein by a double amino acid labeling technique with ³⁵S and ³H as radioactive markers. The isotopic ratio determined for several pairs of amino acids together with the mass and the pI of a given spot is informative enough to find the corresponding open reading frame in a yeast data base

* This work was supported in part by the Groupement de Recherche et d'Études sur les Génomes (GREG) (to J. L. and H. B.) and by the New Jersey Commission for Cancer Research (to M. B. T.). The costs of publication of this article were defrayed in part by the payment of page charges. This article must therefore be hereby marked "advertisement" in accordance with 18 U.S.C. Section 1734 solely to indicate this fact.

** To whom correspondence should be addressed: Service de Biochimie et Génétique Moléculaire, Bât 142, CEA-Saclay, F-91191 Gif-sur-Yvette Cedex, France. Tel.: 33-1-69-08-22-31; Fax: 33-1-69-08-47-12; E-mail: labarre@jonas.saclay.cea.fr.

¹ The abbreviations used are: ROI, redox-active oxygen intermediate; RT, reverse transcription; PCR, polymerase chain reaction.

containing 2700 protein sequences of codon bias index >0.1 with the help of a specific algorithm program. Eight different double labelings were performed here: ³⁵S-Met/³H-Leu, ³⁵S-Met/³H-Lys, ³⁵S-Met/³H-Phe, ³⁵S-Met/³H-Tyr, ³⁵S-Met/³H-Trp, ³⁵S-Met/³H-His, ³⁵S-Cys/³H-Leu and ³⁵S-Cys/³H-His. We analyzed 260 spots out of which 124 already identified spots were used as internal standards for the establishment of calibration curves. Six of these 124 proteins devoid of Cys (Ssc1p, Pgi1p, Hsp12p, Hsp82p, Hsc82p, and Cys3p) were used to estimate the metabolic interconversion of Cys to Met which is about 15%. Reciprocally, two proteins devoid of Met (Tpi1p and Tsa1p) were used to estimate the interconversion from Met to Cys which is about 33%. ³H-Labeled amino acids were chosen among those which are not metabolized into other amino acids in our culture conditions (13). The isotopic ratio obtained for the 124 reference proteins were plotted against their known amino acid ratios taking into account Met and Cys interconversion. Experimental values were in good agreement with the theoretical amino acid ratios. The standard deviation of this analysis ranged from 5 to 18%, depending on the double labeling. These calibration curves were used to determine the 8 amino acid ratios for the other 136 proteins analyzed.

Measurement of the H₂O₂ Response—Mid-log cells (*A*₆₀₀, 0.3) were exposed to H₂O₂ (0.4 mM) at *t* = 0. 2 ml of treated or untreated cultures were then labeled with 500 μCi of [³⁵S]methionine at *t* = 15 min and collected at *t* = 30 min. ³⁵S-Labeled cultures were mixed to an equal aliquot of an ³H-labeled culture just before lysis. This served as an internal standard to correct for any variation in protein yield not attributable to H₂O₂. ³H-Labeled cells were obtained by labeling exponentially growing cells (*A*₆₀₀, 0.3) with [³H]methionine and [³H]leucine for 2 h. Mixtures were then extracted and processed for two-dimensional gel electrophoresis as described previously (13). Gels were then stained with Coomassie Brilliant Blue R-250, dried, and exposed to autoradiography. The more abundant protein spots were numbered, identified on the dried gel, and extracted for counting ³⁵S and ³H emission in a scintillation counter (WALLAC 1409). The ³⁵S/³H ratio of each spot normalized to the ³⁵S/³H Act1p ratio defines the protein synthesis rate index. The ratio of induced to control synthesis rate indexes defines the stimulation (or repression) index. The accuracy of this procedure was demonstrated by comparing two identical uninduced cultures which yielded almost identical results for 400 spots analyzed (S.D. = 0.10). The levels of 111 proteins which differed by a factor of 1.5 or more between uninduced and induced conditions are reported under "Results." The 233 other analyzed protein spots did not significantly change their expression level upon H₂O₂ treatment. Among them, 110 proteins were identified on our two-dimensional maps: ABP1, ACO₂, ACT1, ACT2, ADE1, ADH3, ADK1, APA1, ASN2, ATP14, VMA2, BMH1, BMH2, CCT5, CCT6, CLC1, CMD1, COG1, COR1, CPR1, CPR6, CPR7, CYS4, DAL1, DYS1, EGD1, EGD2, ERG1, FBA1, FRS1, FUM1, GLN1, GND1, GRS1, GSP1, HOM2, HOM6, HSP60, HXK1, HXK2, IDH2, IPP1, KAR2, KRS1, LEU1, LEU2, LPA13, MAS1, MET25, MRP8, NPL3, NTF2, PFK1, PFK2, PFY1, PGI1, PGK1, PRE2, PRE6, PRS4, PSA1, PUB1, PYK1, RBK1, RIB4, RPL1, RPLA3, RPS25A, SBP1, SEC14, SER1, SRP1, SSA4, SSC1, SSE1, SSE2, SUP45, TFP1, TIF11, TIF45, TOM40, TPI1, TPM1, TRP5, TUB2, UBC4, UBC6, UGA1, VMA2, VMA4, YDL100C, YDL161W, YEL047C, YEC071W, YFR044C, YGL245W, YGR012W, YHR064C, YJL068C, YJR105W, YLR192C, YLR206W, YLR301W, YMR116C, YMR120C, YOR007C, YOR230W, YOR280C, YPL088W, YRB1.

Kinetics and Dose-Response Experiments—A mid log culture (*A*₆₀₀, 0.3) was treated at *t* = 0 with H₂O₂ (0.2 mM). Aliquots were then taken at *t* = 1, 2, 7, 11, 19, 36, and 59 min, labeled with 500 μCi of [³⁵S]methionine for 2 min, and then collected, mixed with ³H-labeled cells, and processed as above. Given the 2-min duration of the [³⁵S]methionine pulse, the kinetics experiments corresponded to times 0, 2, 3, 8, 12, 20, 37, and 60 min. For the dose-response analysis, mid log cell cultures (*A*₆₀₀, 0.3) were treated at *t* = 0 with 0, 0.2, 0.4, and 0.8 mM H₂O₂. Cells were then labeled with 500 μCi of [³⁵S]methionine at *t* = 15 min, collected at *t* = 30 min, and processed for two-dimensional gel electrophoresis as described above.

Transcripts Quantification by Northern Analysis and RT-PCR—Exponentially growing cells (*A*₆₀₀, 0.3) were exposed to H₂O₂ (0.2 mM) at *t* = 0 and collected for mRNA preparation at *t* = 0, 15, and 60 min. Cells were disrupted with an Eaton press, and mRNA were extracted with Trizol according to the manufacturer's instructions (Life Technologies, Inc.). mRNA levels were also quantified by a multiplex RT-PCR strategy based on coamplification of specific internal fragments from selected genes using a combination of primers with similar *T_m* and designed to produce different fragment lengths to be resolved on a 4% acrylamide gel. Poly(A)⁺ mRNA were prepared with the poly(A) tract kit (Amer-

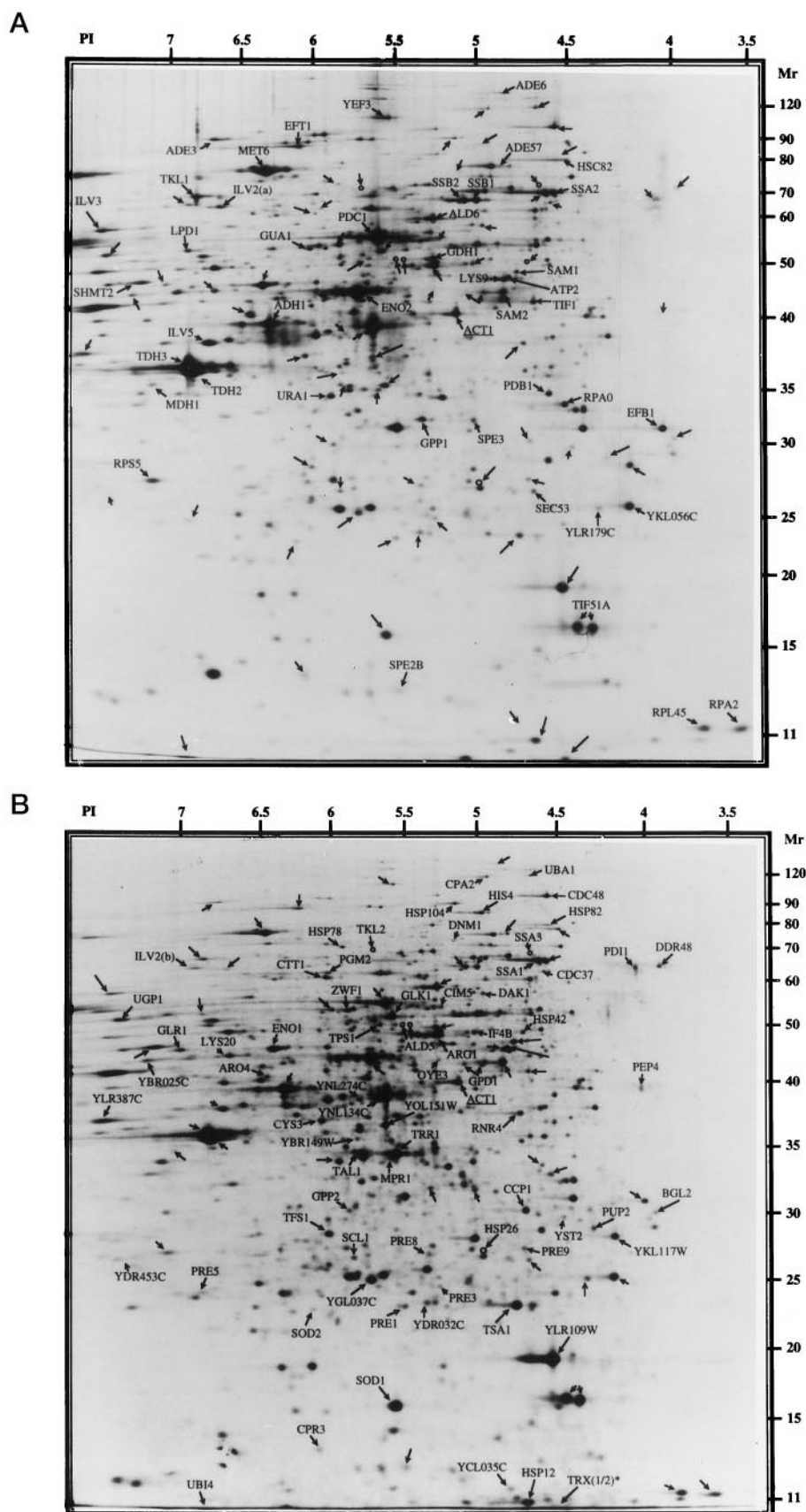
sham Promega Biotech). Double-stranded cDNA libraries were generated from poly(A)⁺ messages with the Life Technologies, Inc. Superscript kit. These cDNA libraries were used in an RT-PCR reaction with appropriate primers and [³³P]dCTP. The labeled RT-PCR products were then resolved by electrophoresis. Gels were dried, exposed to autoradiography, and quantified by phosphor technology (PhosphorImager, Molecular Dynamics). ACT1 RT-PCR products were used as internal standard. All these PCR reactions were in the linear range as attested by comparison to preliminary calibration experiments.

RESULTS

The *S. cerevisiae* Genomic Response to H₂O₂—The exposure of exponentially growing cells to low doses of H₂O₂ results in dramatic changes in protein synthesis. To characterize this oxidative stress genomic response, exponentially growing cells were treated with 0.4 mM H₂O₂ for 15 min and pulse-labeled with [³⁵S]methionine. Labeled extracts from control untreated and treated cells were then subjected to comparative two-dimensional gel electrophoresis (Fig. 1). Changes in the intensity of a number of spots could be recognized by simple visual inspection. We sought to precisely measure these genomic changes. Usual methods rely on the comparative quantification of corresponding ³⁵S-labeled protein spots with a PhosphorImager. However, this method is imprecise at least in part due to differences in the yields of extraction of each protein. To improve this method, we defined an internal protein concentration standard for each spot by adding an equal aliquot of ³H-labeled cells to the ³⁵S-labeled cultures. This allows one to express any change in the rate of protein synthesis as the ratio between the ³⁵S/³H ratios of corresponding spots from two different gels and hence to correct for any variation not related to the H₂O₂ treatment (see "Materials and Methods"). Preliminary experiments comparing two-dimensional gels from two identical cultures showed that the variations observed in the protein quantitation were below a factor of 1.3 for 96% of the 400 control spots analyzed and never exceeded 1.5 (Fig. 2). Therefore, differences by a factor greater than 1.5 between treated and control cultures were considered to be significant. Accordingly, 115 proteins were specifically induced by H₂O₂ with a stimulation index ranging from 1.5 to 20 (see Table I). Conversely, 52 other proteins were repressed with a repression index ranging from 0.65 to 0.15 (Table I). Almost identical results were observed with two related yeast strains S288C and YPH98.

Proteins Induced by H₂O₂—The identity of 71 of the 115 proteins induced by H₂O₂ is given in Table I along with their stimulation index. 39 of them were previously identified on two-dimensional maps (for review, see Ref. 17). The 32 other spots were identified in this work by amino acid analysis as described by Mailliet *et al.* (13) or by mass spectrometry (16). H₂O₂-responsive proteins were sorted into seven different functional classes (see Table I). (i) Proteins directly related to the cellular antioxidant defense: This class shows a high stimulation index which ranges from 3 to 20 depending on the protein. It comprises the major oxidant scavenging enzymes cytochrome *c* peroxidase (Ccp1p), cytosolic catalase (Ctt1p), Cu/Zn and Mn superoxide dismutases (Sod1p and Sod2p), thioperoxidase (Tsa1p), thioredoxin (Trx1p or Trx2p), NADPH-dependent thioredoxin reductase (Trr1p), and glutathione reductase (Glr1p). Four newly identified proteins were included in this functional class on the basis of their homology to known oxidant scavenging enzymes and/or suspected antioxidant defense properties. YDR453Cp is one of the two other AhpC/TSA family members identified in the yeast genome. YCL035Cp is 86% similar and 68% identical to *TTR1*-encoded glutaredoxin (thioltransferase). YLR109Wp and YOL151Wp were classified here on the basis of their role in the tolerance to *tert*-butyl hydroperoxide and diamide, respectively (see "Discussion"). (ii) Heat shock proteins:

FIG. 1. Comparative two-dimensional gel electrophoresis of total yeast proteins before and after H₂O₂ treatment. Autoradiograms of two-dimensional gel electrophoresis performed with total yeast extracts from [³⁵S]methionine-labeled cells as described under "Materials and Methods." Proteins whose synthesis rate was changed by a factor of 1.5 or more upon H₂O₂ exposure are indicated by their name and an *arrow*. Notice the presence of two spots corresponding to Ilv2p, Ilv2p(a) and Ilv2p(b). The internal standard Act1p is also indicated. **A**, extracts prepared from control untreated cells. The proteins named here are those repressed by H₂O₂. **B**, extracts prepared from cells exposed to H₂O₂ (0.4 mM) for 15 min. The proteins named here are those stimulated by the H₂O₂ exposure. *o*, some proteins are not visible on these maps either because they are only expressed at higher H₂O₂ concentrations (Ald5p, Tkl2p) or because they do not contain sulfur amino acids (Hsp26p).



This class also shows a strong stimulation index for several of its members. (iii) Proteases and proteasome subunits: The stimulation index is significant but not as high as in the two previous classes. (iv) Translation apparatus components: This

class contains only two H₂O₂-inducible proteins but several H₂O₂-repressed targets (see below). (v) Carbohydrate metabolism enzymes. (vi) Enzymes involved in amino acid metabolism. (vii) Unclassified proteins and open reading frames of unknown

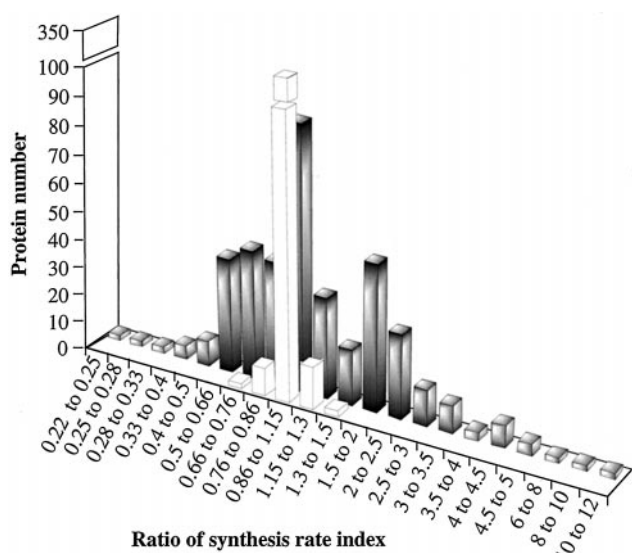


FIG. 2. Histogram indicating the distribution of the changes in synthesis rate index for 400 proteins. The synthesis rate index was calculated as described under "Materials and Methods." White bars, differences observed in the synthesis rate index of 400 proteins in duplicate experiments performed in identical conditions with extracts from control untreated cultures. These differences actually reflect the experimental error associated with the procedure. Black bars, changes observed in the synthesis rate index of 400 proteins between a control untreated and a culture exposed to H₂O₂ (0.4 mM) for 15 min.

function: These include two putative regulators, Cdc37p and Mpr1p. *MPR1* is the *S. cerevisiae* homologue of *Schizosaccharomyces pombe* *Pad1+*, a global positive regulator of transcription implicated in chromatin structure and identified as a positive regulator of Pap1p, the *S. pombe* homologue of Yap1p (18). Cdc37p has been shown to be a chaperone acting with Hsp90p and other chaperones to promote the folding/activity of a series of kinases (19).

Proteins Repressed by H₂O₂—44 out of these 52 proteins had been previously identified on two-dimensional maps (17). Each was assigned a repression factor and sorted into functional classes (Table I). Most of these proteins are translational apparatus components and metabolic enzymes. They include the translation initiation factors eIF4A (Tif1p) and eIF5A (Tif51Ap) and the translation elongation factors EF1-β (Efb1p), EF-2 (Eft1p), and EF-3 (Yef3p), which are dramatically repressed. Rpa0p, Rpa2p, Rpa4p, and Rps5p are acidic ribosomal proteins that act both at the initiation and the elongation steps (20). Ssb1p and Ssb2p are heat shock proteins of the 70-kDa superfamily that are ribosomal-associated and have a role in the folding of nascent polypeptides emanating from the ribosome (21, 22). Metabolic enzymes repressed by H₂O₂ include enzymes involved in glycolysis, the Krebs cycle, purine and amino acid biosynthesis, sulfur metabolism, *S*-adenosylmethionine, and polyamine biosynthesis. Ilv2p(a) (acetolactate synthase) appears repressed by a factor of 0.35. Interestingly, we could identify a H₂O₂-responsive spot of pI 6.7 and *M_r* 67,000 with a very good match with Ilv2p with regard to its amino acid composition, and therefore it is indicated as Ilv2p(b) in Fig. 1 (13). It may represent an Ilv2p precursor form. The apparent Ilv2p repression seen here may thus be related to the decreased maturation/mitochondrial translocation of its precursor. The remaining eight H₂O₂-repressed targets have not yet been identified.

Kinetics and Dose-Response Profiles of the H₂O₂ Response—The kinetics of the genomic response to H₂O₂ was analyzed for 36 H₂O₂-responsive targets by pulse-labeling cells for 2 min at various times after the H₂O₂ treatment. Two-dimensional gel

electrophoresis was then performed to determine the relative rate of synthesis of several proteins. Except for a few targets, the H₂O₂ response was very rapid and transient. We could define three kinetic classes (Fig. 3A). Proteins of class A responded as early as 2 min after induction with a peak at approximately 15 min and a complete return to the base line after 1 h. Proteins of class B had a very similar kinetic profile but initiated their response with a lag period of at least 4 min. Class c proteins had a somewhat different kinetic profile with a relatively delayed response and a peak at 45 min or even at 1 h for Uba1p. Repression by H₂O₂ was similarly transient with a nadir at approximately 15 min after stress imposition.

We also tested the H₂O₂ dose-genomic response profile (Fig. 4). Synthesis rates were determined 15 min after exposure to 0.2, 0.4, or 0.8 mM H₂O₂ for 61 H₂O₂-responsive targets. Trr1p and several other proteins were equally induced by each of the three H₂O₂ doses tested (Fig. 4). Interestingly, Ccp1p and several other proteins were maximally induced by 0.2 mM H₂O₂. In contrast, most of the heat shock proteins exhibited their maximal response at 0.8 mM. These kinetics and dose-response differences may be related to distinct regulatory mechanisms.

Alterations in mRNA Levels and Protein Synthesis Rates Are Parallel after H₂O₂ Treatment—The alterations observed in the expression of target proteins in response to H₂O₂ are likely to include a transcriptional component. We therefore evaluated the mRNA levels of eight selected H₂O₂-responsive targets. Total poly(A) transcripts were purified from control untreated cells and from cells treated with 0.4 mM H₂O₂ for 15 or 60 min and quantified by PCR. The results for *TRR1*, *CCP1*, *YDR453C*, *YNL134C*, and *YOL151W* are shown in Fig. 5. Levels of all the transcripts analyzed were increased by 5–37-fold at 15 min after H₂O₂ exposure and had returned close to their basal levels at 60 min. We also analyzed by Northern blot the kinetic profile of the *TRR1* message levels at several points after H₂O₂ treatment (Fig. 3B). The kinetics of the message levels and protein synthesis rates are strikingly parallel after H₂O₂ treatment. These data corroborate those obtained from the two-dimensional gel analysis and strongly suggest that the dramatic genomic response to H₂O₂ involves, at least in part, a transcriptional control.

DISCUSSION

ROI are obligate by-products of aerobic life which can inflict structural damage to a wide variety of cell components, thus leading to oxidative stress and cell death. Stress-inducible defense or adaptive response mechanisms act to protect cells from these oxidative threats (2, 4, 5). For instance, the exposure of bacteria or yeast to low levels of H₂O₂- or O₂⁻-generating drugs switches on within minutes a resistance to toxic doses of these oxidants. These adaptative stress responses are produced by the induction of distinct batteries of genes or stimulons. However, the genes which constitute these stimulons are, for the most part, not yet identified. We have attempted here a systematic identification of the gene products of the *S. cerevisiae* H₂O₂ stimulon. An intense gene activity occurs within minutes of exposure to H₂O₂, resulting in a transient alteration in the synthesis of at least 150 proteins. The identification of 71 stimulated and 44 repressed proteins and their assignment to specific cellular processes has given a distinct picture of the way in which yeast cells adapt to oxidative stress. The cellular functions that are primarily affected by these changes are antioxidant defenses, heat shock and chaperone proteins, translational apparatus, proteases, and carbohydrate metabolism.

Antioxidant Defense Activities—As expected, several primary antioxidants were induced by H₂O₂. They include cyto-

TABLE I
 Identification of 71 proteins stimulated and 44 repressed by H₂O₂

Gene name	Repression ^a	Induction ^b	Protein function
I. Proteins with antioxidant scavenging/defense properties			
CCP1		6	Cytochrome c peroxidase
CTT1		14.7	Catalase T ^c
GLR1		2.1	Glutathione reductase ^{c,d}
SOD1		4.3	Cu/Zn superoxide dismutase
SOD2		5.9	Mn superoxide dismutase
TRR1		12.2	Thioredoxin reductase/NADPH dependent ^c
TRX (1/2)		11.5	Thioredoxin 1 or 2 ^c
TSA1		5.9	Thiol-specific antioxidant protein/thioperoxidase
YCL035C		5	Similarity to thioltransferase (glutaredoxin) ^c
YDR453C		>15	Similarity to Tsa1p ^c
YLR109W		3.1	Similarity to C, bovidini peroxisomal protein A and B
YOL151W		5.9	Similarity to plant dihydroflavonol-4-reductases ^c
II. Heat shock and chaperone proteins			
CPR3		2.3	Cyclophilin ^c
DDR48		7.4	Heat, salt, and DNA damage inducible
HSC82	0.62		82-kDa heat shock protein
HSP104		14.9	104-kDa heat shock protein
HSP12		10	12-kDa heat shock protein ^c
HSP26		>5	26-kDa heat shock protein
HSP42		4	42-kDa heat shock protein ^c
HSP82		2.3	82-kDa heat shock protein
PDI1		2.8	Protein-disulfide isomerase
SSA1		2.7	Heat shock protein
SSA2	0.33		Heat shock protein
SSA3		4.2	Heat shock protein
III. Proteases			
CIM5		1.7	Proteasome subunit
PRE1		2.3	Proteasome subunit ^c
PRE3		1.9	Proteasome subunit
PRE5		3.4	Proteasome subunit ^c
PRE8		1.5	Proteasome subunit
PRE9		2	Proteasome subunit
PUP2		2.9	Proteasome subunit ^c
SCL1		2.5	Proteasome subunit ^c
UBA1		1.6	Ubiquitin-activating enzyme
UB14		1.75	Ubiquitin ^c
HSP78		4.9	Mitochondrial protease ^c
PEP4		2.9	Vacuolar protease A
IV. Protein translation apparatus			
EFB1	0.12		Translation elongation factor EF-1β
EFT1	0.21		Translation elongation factor EF-2
YEF3	0.11		Translation elongation factor EF-3
IF4B		>2	Translation initiation factor eIF4B ^d
TIF1	0.42		Translation initiation factor eIF4A
TIF51A	0.52		Translation initiation factor eIF5A
RPS5	0.5		Ribosomal protein RPS5
YST2		1.9	Ribosomal protein
RPA2	0.17		Acidic ribosomal protein L44
RPA0	0.65		Acidic ribosomal protein A0
RPL45	0.36		Acidic ribosomal protein L45
SSB1	0.16		Heat shock protein family
SSB2	0.18		Heat shock protein family
Not classified			
ATP2	0.64		ATP synthase
BGL2		2.4	β-Glucanase
CDC48		1.5	ATPase Family
DNM1		6.2	Dynammin-related protein ^c
OYE3		2.1	NADPH dehydrogenase ^d
RNR4		2.2	Ribonucleotide reductase small subunit
YBR025C		6.4	Strong similarity to Yif1p
YKL056C	0.42		Translationally controlled tumor protein (TCTP)
TFS1		9.7	Suppressor of cdc25 mutation ^c
YLR179C	0.53		Similarity to Tfs1p
V. Carbohydrate metabolism enzymes			
Pentose phosphate pathway			
TAL1		4.1	Transaldolase ^c
TKL1	0.2		Transketolase
TKL2		3.9	Transketolase ^c
ZWF1		2	Glucose-6-phosphate dehydrogenase
Glycolysis			
ADH1	0.63		Alcohol dehydrogenase
ALD5		2.1	Aldehyde dehydrogenase
ALD6	0.52		Aldehyde dehydrogenase
ENO1		1.6	Enolase
ENO2	0.37		Enolase
GLK1		3.8	Glucokinase

TABLE I—continued

Gene name	Repression ^a	Induction ^b	Protein function
PDC1	0.27		Pyruvate decarboxylase
SEC 53	0.31		Phosphomannomutase
TDH 2	0.59		Glyceraldehyde-3-phosphate dehydrogenase
TDH 3	0.47		Glyceraldehyde-3-phosphate dehydrogenase
Trichloroacetic acid cycle			
LPD1	0.45		Dihydrolipoamide dehydrogenase
MDH1	0.6		Malate dehydrogenase
PDB1	0.34		Pyruvate dehydrogenase
Glycerol metabolism			
DAK1		3	Similarity to dihydroxyacetone kinase
GPD1		2.6	Glycerol phosphate dehydrogenase
GPP1	0.55		Glycerol phosphate phosphatase
GPP2		1.5	Glycerol phosphate phosphatase ^c
YBR149W		1.7	Glycerol dehydrogenase
Trehalose synthesis			
PGM2		4.4	Phosphoglucomutase
TPS1		3.8	Trehalose-6-phosphate synthase
UGP1		>2	UDP-glucose pyrophosphorylase
VI. Sulfur, amino acids, and purine metabolism enzymes			
Sulfur metabolism			
CYS3		3.2	Cystathionine γ -lyase
MET6	0.22		Methionine synthase
SAM1	0.42		S-Adenosylmethionine synthetase 1
SAM2	0.48		S-Adenosylmethionine synthetase 2
Polyamine pathway			
SPE2B	0.25		S-Adenosylmethionine decarboxylase α chain ^c
SPE3	0.53		Spermidine synthase ^c
Amino acids metabolism			
ARG1		3.1	Arginosuccinate synthase
ARO4		3.1	2-Dehydro-3-deoxyphosphoheptonate aldolase
CPA2		2.1	Carbamyl phosphate synthase
GDH1	0.36		Glutamate dehydrogenase (NADP ⁺)
HIS4		2.3	AMP cyclohydrolase
ILV2 (a)	0.31		Acetolactate synthase
ILV2 (b)		2	Acetolactate synthase ^c
ILV3	0.6		Dihydroxyacid dehydratase ^c
ILV5	0.15		Acetohydroxyacid reductoisomerase
LYS20		1.8	Probable homocitrate synthase ^c
LYS9	0.55		Saccharopine dehydrogenase (NADP ⁺)
SHMT2	0.44		Serine hydroxymethyltransferase
Purine and pyrimidine synthesis			
GUA1	0.48		GMP synthetase
ADE3	0.32		C1-tetrahydrofolate synthase
ADE6	0.55		5'-Phosphoribosylformylglycinamide synthase
ADE57	0.28		Phosphoribosylamine-glycine ligase and phosphoribosylformylglycinamide cyclo-ligase
URA1	0.45		Dihydroorotate dehydrogenase ^d
Regulatory proteins			
CDC37		1.5	Kinase regulator
MPR1		3.1	Similarity to <i>S. pombe</i> Pad1p ^c
Unknown function			
YDR032C		2.5	Strong similarity to <i>S. pombe</i> Obr1 ^c
YGL037C		6.8	^c
YKL117W		2.3	Ste5p-associated protein
YLR387C		1.6	Protein with zing finger domain ^c
YNL134C		2.6	^c
YNL274C		2.1	Similarity to α -ketoisocaproate reductase ^d

^a Repression indexes recorded here were determined in response to 0.4 mM H₂O₂.

^b Stimulation indexes were determined in response to 0.2, 0.4, and 0.8 mM H₂O₂ and the highest value was recorded.

^c Proteins identified during this work by the double labeling method.

^d Proteins identified by mass spectrometry.

chrome *c* peroxidase, cytosolic catalase, superoxide dismutases, thioperoxidase (Tsa1p), thioredoxin 1 or 2, NADPH-dependent thioredoxin reductase, and NADPH-dependent glutathione reductase. Antioxidant defense properties have been reported in yeast for all these genes except cytochrome *c* peroxidase (23–30). We have also identified four new proteins with possible antioxidant defense properties. YDR453C is one of the other AhpC/TSA homologues discovered in the yeast genome sequencing project. YDR453C and Tsa1p are 96% similar and 86% identical. They share N-terminal and C-terminal catalytic cysteines of the AhpC/TSA homology (27). YDR453C is likely to carry the antioxidant function described for Tsa1p, which in-

volves the reduction of peroxides with electrons donated by thioredoxin, thioredoxin reductase, and NADPH (28). YLR109W is a new antioxidant related to the peroxiredoxin AhpC/TSA protein family and is quite similar to peroxisomal membrane proteins (PMP20) A and B of *Candida boydii* (31). YLR109W displays defense activity against *tert*-butyl hydroperoxide² and represents a subclass of the AhpC/TSA protein family localized in the peroxisome. YCL035C is very homologous to glutaredoxin encoded *TTR1* (32) and carries both cysteine signatures of the glutaredoxin/thioltransferase family

² J. Lee, unpublished results.

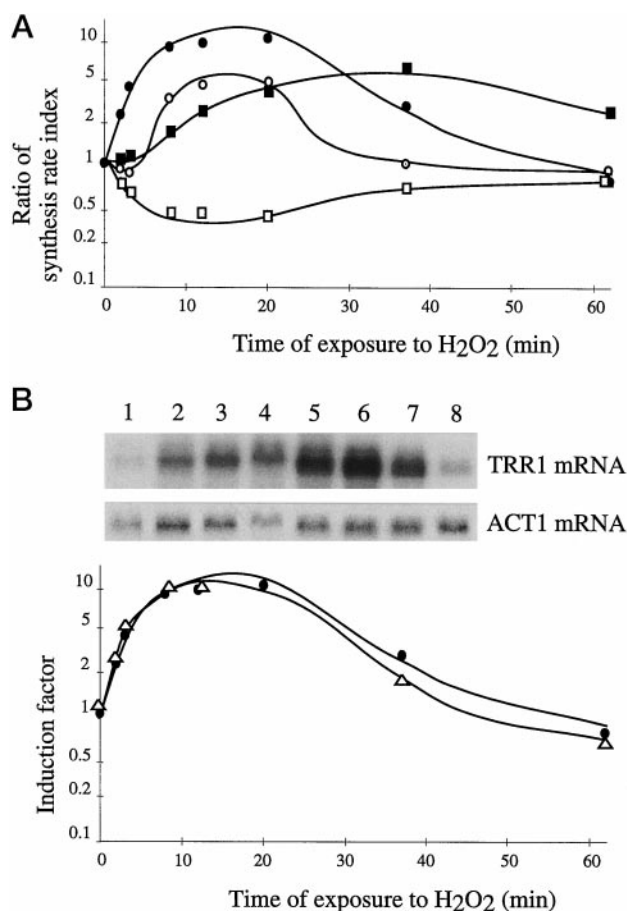


FIG. 3. Kinetics of the H₂O₂ response. A, protein kinetic profiles. The synthesis rate index of 36 H₂O₂-responsive targets were calculated as described under "Materials and Methods" from two-dimensional gel electrophoresis performed with control untreated cells or with cells treated with H₂O₂ (0.2 mM) for 1, 2, 7, 11, 19, 36, and 59 min. A representative profile of each of the three kinetic classes is given. Class a: *Trr1p* (filled circles), *Ddr48p*, *Sod1p*, *Trx1/2p*, *Tsa1p*, *YBR025C*, *YDR353W*, *YLR109W*, and *YOL151W*. Class b: *Ctt1p* (open circles), *Arg1p*, *Aro4p*, *Ccp1p*, *Cpa2p*, *Glr1p*, *Glk1p*, *Mpr1p*, *Sod2p*, *Tfs1p*, *YGL037C*, and *YNL134C*. Class c: *Hsp12p* (filled squares), *Cdc48*, *Eno1p*, and *Uba1p*. Repressed proteins: *Efb1p* (open square), *Ade57p*, *Eft1p*, *Gdh1p*, *Ilv5p*, *Met6p*, *Rpa2p*, *Sec53p*, *Spe2Bp*, *Ssb1p*, and *Ssb2p*. B, *TRR1* mRNA kinetic profile. Total mRNA were isolated from control untreated cells (lane 1), and from cells treated with H₂O₂ (0.2 mM) for 1, 2, 7, 11, 19, 36, and 59 min (lanes 2–8). The Northern blot was hybridized with a *TRR1* and an *ACT1* probe which served as a control. The *TRR1* message levels were quantified with a PhosphorImager, normalized to the *ACT1* mRNA, and plotted (open triangles). On the same graph is plotted the kinetics of the synthesis rate index of *Trr1p* at identical time point after exposure H₂O₂ (filled circles).

redox center. YOL151W is similar to NADPH dihydroflavonoid reductases involved in the plant synthesis of isoflavonoid phytoalexins. The antioxidant defense properties of these reductases were demonstrated by the isolation of an isoflavonoid reductase gene from an *Arabidopsis thaliana* cDNA library in a search for activities able to rescue the diamide hypersensitivity phenotype of a yeast strain deleted for the oxidative stress response regulator *YAP1* (33). YBR149W is related to aldo/keto reductases and may act as an NADPH-dependent aldehyde reductase to scavenge lipid peroxidation-derived toxic aldehydes by their reduction into alcohols (34, 35). However, YBR149W could also act as an NADP⁺-dependent glycerol dehydrogenase (see below). Although its product could not be detected in our two-dimensional gels maps, *GSH1* (γ -glutamyl-cysteine synthase) mRNA levels are dramatically increased by H₂O₂ (data not shown) and is therefore a part of the H₂O₂ stimulon.

Heat Shock Proteins, Proteases, and the Translation Apparatus—Twelve heat shock proteins (HSP) as well as proline isomerase (*Cpr3p*) and protein disulfide isomerase (*Pdi1p*) were identified as H₂O₂-inducible targets. HSPs are induced in response to a wide variety of stress conditions and are important for the protection of cells from these adverse conditions (reviewed in Refs. 21, 36, and 37). Most of the HSPs are molecular chaperones that assist abnormal proteins accumulating under stress conditions to regain their proper folding or help their proteolytic degradation. The H₂O₂ induction of several

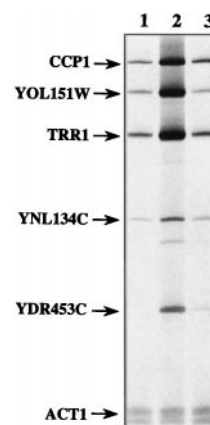


FIG. 5. Changes in mRNA levels in response to H₂O₂. The changes in the mRNA levels of selected targets in response to H₂O₂ were monitored by RT-PCR. mRNA templates used in the RT-PCR reactions were obtained from control untreated cells (lane 1), and from cells exposed to H₂O₂ (0.2 mM) for 15 min (lane 2) or 60 min (lane 3). *ACT1* served as a control. Each RT-PCR product is identified at the left of the autoradiogram.

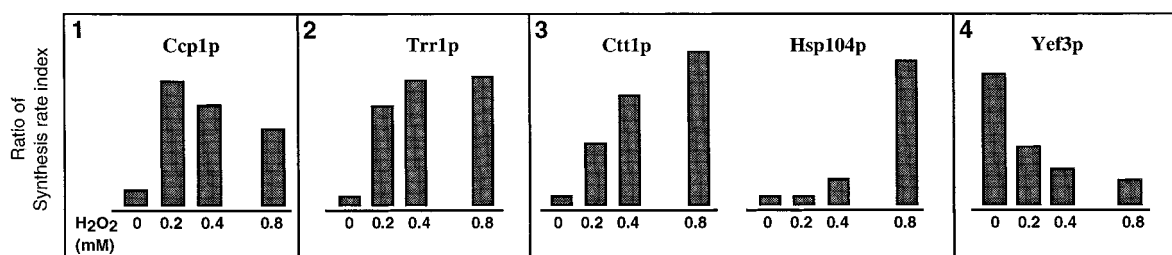
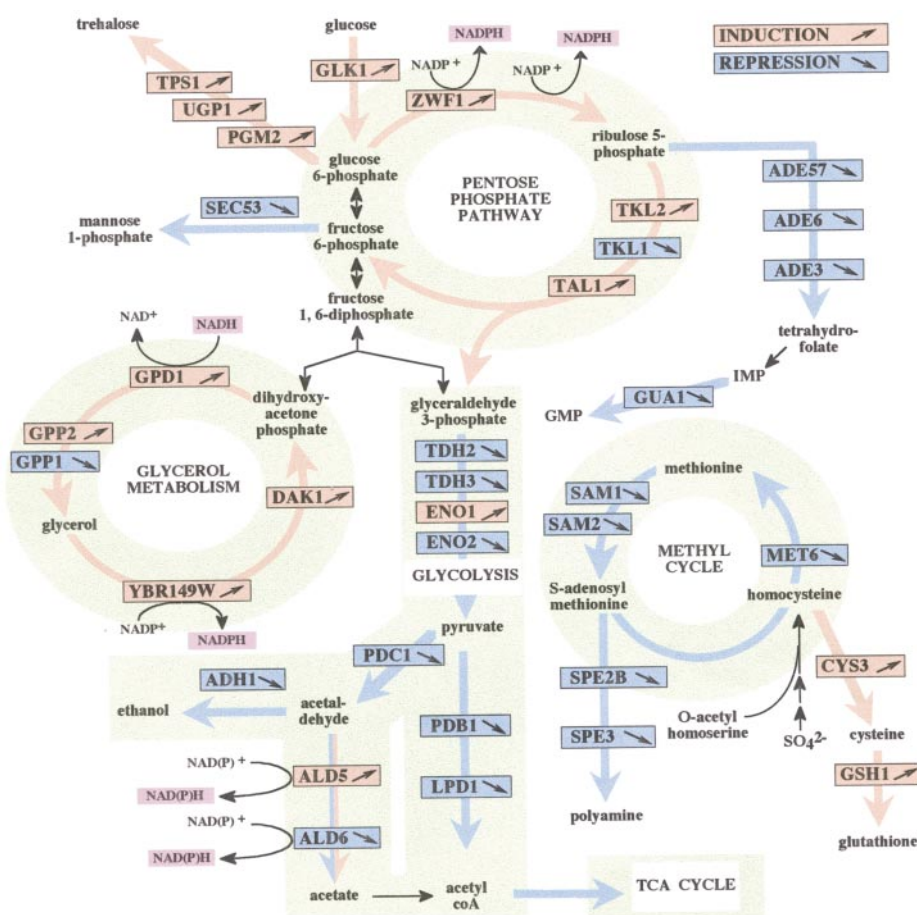


FIG. 4. H₂O₂ dose-response profiles. The synthesis rate index of 61 H₂O₂-responsive targets were calculated, as described in methods, from two-dimensional gels performed with control untreated cells or with cells treated with 0.2, 0.4, or 0.8 mM H₂O₂. A representative dose-response graph is given for each of the three groups individualized and for the repressed proteins. Class 1, *Ccp1p*, *Arg1p*, *His4p*, *Sod2p*, and *YBR025C*. Class 2, *Trr1p*, *Cim5p*, *Ddr48p*, *Glk1p*, *Glr1p*, *Mpr1p*, *Sod1p*, *Trx1/2p*, *Tsa1p*, *Zwf1p*, *YDR453C*, *YNL134C*, and *YOL151W*. Class 3, *Ctt1p*, *Hsp104p*, *Ald5p*, *Bgl2p*, *Cpr3p*, *Cys3p*, *Dak1p*, *Hsp12p*, *Hsp42p*, *Hsp78p*, *Ilv2p(b)*, *Pdi1p*, *Pep4p*, *Pgm2p*, *Pre3p*, *Rnr4p*, *Scl1p*, *Ssa1p*, *Ssa3p*, *Tfs1p*, *Tps1p*, *YCL035C*, *YGL037C*, and *YLR109W*. Repressed proteins: *Yef3p*, *Efb1p*, *Eft1p*, *Eno2p*, *Ilv2p(a)*, *Ilv5p*, *Met6p*, *Pdb1p*, *Pdc1p*, *Rpa2p*, *Rpl45p*, *Sam1p*, *Sam2p*, *Sec53p*, *Ssb1p*, *Ssb2p*, *Tdh3p*, *eIF4A*, and *eIF5A*.

FIG. 6. **Metabolic pathways altered during the H₂O₂ response.** Only H₂O₂-responsive proteins are mapped, with those induced framed in red and those repressed framed in blue. TCA, trichloroacetic acid.



subunits of the proteasome along with enzymes of the ubiquitin pathway, mitochondrial and lysosomal proteases is also consistent with an important proteolytic activity during the oxidative stress response. Induction of the ubiquitin pathway by oxidative stress and the specific degradation of oxidized proteins by the proteasome has been recently demonstrated (38, 39). Most of the chaperones and proteases have essential roles under nonstress conditions by assisting protein biogenesis, oligomer assembly, traffic between cellular organelles, and selective protein degradation (40, 41). Hence, in addition to their protective functions, they may help to reorchestrate the cell metabolism to the needs of the oxidative stress response. Associated with these changes, the repression of two translation initiation and four translation elongation indicates a global and nonspecific slowdown of protein translation. We could indeed demonstrate a 2.5-fold decrease of translation in response to 0.3 mM H₂O₂ by [¹⁴C]leucine labeling (data not shown). Taken together, the response of HSPs, proteases, and the translational apparatus to H₂O₂ is probably important for switching the cellular activity from biosynthetic toward protective functions.

Carbohydrate Metabolism and NADPH Regeneration— Twenty-five H₂O₂-responsive targets were identified as metabolic enzymes. Although not exhaustive, this identification provides an indication of the metabolic fluxes redistribution occurring in response to H₂O₂. These changes dramatically affect carbohydrate metabolism which appears to be diverted to the generation of NADPH, the most important cellular reducing power (Fig. 6). (i) The hexose monophosphate pool: Repression of phosphomannomutase (Sec53p), stimulation of phosphoglucomutase (Pgm2p), and exclusion of glucose from glycolysis (see below) seem to redirect the hexose phosphate pool to the pentose phosphate pathway and the trehalose syn-

thesis. (ii) Induction of trehalose synthesis: Trehalose synthesis is stimulated by oxidative stress as indicated by the induction of phosphoglucomutase (Pgm2p), UDP-glucose pyrophosphorylase (Ugp1p), and trehalose-6-phosphate synthase (Tps1p). Trehalose synthesis is also stimulated by heat shock and osmotic stress (42–44), and its accumulation correlates with thermotolerance (45). Parrou *et al.* (46) also observed the induction of *TPS1* by H₂O₂ but curiously without any trehalose accumulation. We also could not detect any change in trehalose steady state and synthesis rate levels by [¹⁴C]glucose labeling (data not shown). These data suggest the existence of an enhanced recycling of this disaccharide (46, 47). (iii) Induction of the pentose phosphate pathway: Three enzymes of the pentose phosphate pathway are induced by H₂O₂. Glucose-6-phosphate dehydrogenase (Zwf1p) regulates the carbon flow through this pathway by catalyzing its first step, leading to ribulose 5-phosphate, the precursor of purine biosynthesis (48). Then, pentose phosphates are interconverted to glyceraldehyde 3-phosphate or fructose 6-phosphate by transketolases (Tkl1p and Tkl2p) and transaldolase (Tal1p). Glyceraldehyde 3-phosphate can enter glycolysis and fructose 6-phosphate is converted to glucose 6-phosphate (49). However, repression of glycolysis (see below) and purine biosynthesis pathway suggest that most of the pentose phosphates are recycled to the hexose phosphate pool for NADPH production. (iv) Repression of glycolysis: H₂O₂ treatment results in a slowdown of glycolysis as manifested by repression of Tdh2p and Tdh3p, and the isozymes of both enolase and pyruvate decarboxylase. (v) Repression of the tricarboxylic acid cycle: The decreased expression of pyruvate decarboxylase and pyruvate dehydrogenase, the two enzymes which catalyze the alternative entries into the trichloroacetic acid cycle suggests a further slowdown of the trichloroacetic acid cycle, which is already subject to catabolite repression.

Repression of malate dehydrogenase (Mdh1p) is also consistent with this notion. (vi) Alteration of glycerol metabolism: Glycerol synthesis must be increased in response to H₂O₂ as suggested by the induction of glycerol phosphate dehydrogenase (Gpd1p) and glycerol phosphate phosphatase (Gpp2p) (Table I). In addition, Dak1p, a dihydroxyacetone kinase and YBR149Wp, a putative glycerol dehydrogenase, which have been assigned to a new salt-induced glycerol dissimilation pathway (50) are also induced by H₂O₂. This glycerol cycle composed of Gpd1p, Gpp2p, YBR149Wp, and Dak1p (Fig. 6) may function as a transhydrogenase activity to convert NADH to NADPH at the expense of one ATP (50).

In conclusion, the carbohydrate metabolism alteration seems to principally concur to the regeneration of NADPH. NADPH is important in the oxidative stress response as a cofactor for glutathione reductase and thioredoxin reductase, two critical activities in the cellular thiol redox control and antioxidant defense (28, 29, 52). The critical role of NADPH is also suggested by the H₂O₂ hypersensitivity of strains mutated for any of the six enzymes of the pentose phosphate pathway (51, 53) and by the capacity of *TKL1* overexpression to suppress the oxygen sensitivity of a *sod1* null mutant (54). Studies with cells carrying a genetic ablation of the pentose phosphate pathway have also suggested that other cellular mechanisms of NADPH production must exist (51, 53, 55). The glycerol dissimilation pathway might be such a mechanism of NADPH regeneration.

Large Scale Analysis of Gene Expression—We have analyzed the global changes in protein expression underlying the yeast adaptive stress response to H₂O₂ by a two-dimensional gel approach. Although very informative, this analysis is limited by the fact that only soluble and abundant proteins are seen on two-dimensional gels. Membrane-bound proteins or those with a very low or very high molecular weight or with a pI higher than 7.5 are not observed. Based on the expression of about 4500–5000 genes under normal growth conditions (56) and on the detection of about 1000 two-dimensional gel spots, we estimate to have covered about 20% of all expressed proteins. Brown and colleagues (57) have described a new method for the monitoring of gene expression on a genomic scale with a DNA microarray technique which covers the entire yeast genome. This approach monitors changes in mRNA levels for the entire yeast genome, but cannot reveal translational or post-translational control mechanisms. Furthermore, highly homologous isogenes are more readily differentiated by their protein products than by nucleic acid hybridization pattern. Although we observed the concordant alteration in the expression of several isogenes (*Sod1p/Sod2p*, *Tsa1p/YDR453*, *Ssb1p/Ssb2p*, *Sam1p/Sam2p*), we also observed that several other isogenes were differentially expressed during the oxidative stress response (*Tkl1p/Tkl2p*, *Ald5p/Ald6p*, *Ssa1p/Ssa2p*, *Hsc82p/Hsp82p*, *Gpp1p/Gpp2p*, *Tfs1p/YLR179C*). Such differential expression of specific isozymes has also been observed with a two-dimensional gel approach by Norbeck and Blomberg (50), but its physiological meaning is not understood. In summary, we think that the power of the DNA microarray technique in the genomic scale analysis of gene expression should be complemented by the more limited but more biochemical two-dimensional gel approach that allows visualization of post-transcriptional modifications.

Perspectives—The rapid and widespread genomic response to H₂O₂ seen here must involve several inducible control mechanisms. These mechanisms could be, at least in part, transcriptional as suggested by the good correlation between mRNA and protein levels for several of the targets analyzed. Our experimental system provides us a unique opportunity to identify the genetic circuitry that regulates and executes the adaptive re-

sponse to H₂O₂. Several regulators suspected to play a role in the yeast H₂O₂ response include Yap1p and Skn7p (30, 58–60), Msn2p/4p (61), Hsf1p (62), and Gcn4p (63). The assignment of their respective targets to each of these regulators will help to define the different regulons involved in the oxidative stress response.

Acknowledgments—We are grateful to J. Garin for mass spectrometry analysis, E. Leonce and A. Valleix for scintillation counting, and A. Boudsocq for amino acid analysis. We thank Y. Kerjan and D. Thomas for fruitful discussions, D. Spector and C. Mann for critical reading of the manuscript, and P. Thuriaux and A. Sentenac for encouragement and critical discussions.

REFERENCES

- Halliwell, B., and Gutteridge, J. M. C. (1989) *Free Radicals in Biology and Medicine*, pp. 1–85, Clarendon Press, Oxford, UK
- Storz, G., Tartaglia, L. A., Farr, S. B., and Ames, B. N. (1990) *Trends Genet.* **6**, 363–368
- Halliwell, B. (1994) *Nutr. Rev.* **52**, 253–265
- Crawford, D. R., and Davis, K. J. A. (1994) *Environ. Health Perspect.* **102**, 25–28
- Demple, B., and Amabile-Cuevas, C. F. (1991) *Cell* **67**, 837–839
- Kullik, I., and Storz, G. (1994) *Redox Rep.* **1–7**,
- Flattery-O'Brien, J., Collinson, L. P., and Dawes, I. W. (1993) *J. Gen. Microbiol.* **139**, 501–507
- Jamieson, D. J. (1992) *J. Bacteriol.* **174**, 6678–6681
- Collinson, L. P., and Dawes, I. W. (1992) *J. Gen. Microbiol.* **138**, 329–335
- Jamieson, D. J., Rivers, S. L., and Stephen, D. W. S. (1994) *Microbiology* **140**, 3277–3283
- Gralla, E. B., and Kosman, D. J. (1992) *Adv. Genet.* **30**, 251–319
- Moradas-Ferreira, P., Costa, V., Piper, P., and Magner, W. (1996) *Mol. Microbiol.* **19**, 651–658
- Maillet, I., Lagniel, G., Perrot, M., Boucherie, H., and Labarre, J. (1996) *J. Biol. Chem.* **271**, 10263–10270
- Sikorski, R. S., and Hieter, P. (1989) *Genetics* **122**, 19–27
- Mortimer, R. K., and Johnston, J. R. (1986) *Genetics* **113**, 35–43
- Shevshenko, A., Wilm, M., Vorm, O., and Mann, M. (1996) *Anal. Chem.* **68**, 850–858
- Boucherie, H., Sagliocco, F., Joubert, R., Maillet, I., Labarre, J., and Perrot, M. (1996) *Electrophoresis* **17**, 1683–1699
- Shimanuki, M., Saka, Y., Yanagida, M., and Toda, T. (1995) *J. Cell Sci.* **108**, 569–579
- Stepanova, L., Leng, X., Parker, S. B., and Harper, J. W. (1996) *Genes Dev.* **10**, 1491–1502
- Ramacha, M., Jimenez-Diaz, A., Bermejo, B., Rodriguez-Gabriel, M. A., Guarinos, E., and Ballesta, J. P. (1995) *Mol. Cell. Biol.* **15**, 4754–4762
- Craig, E. A., Gambill, B. D., and Nelson, R. J. (1993) *Microbiol. Rev.* **57**, 402–414
- James, P., Pfund, C., and Craig, E. A. (1997) *Science* **275**, 387–389
- Izawa, S., Inoue, Y., and Kimura, A. (1996) *Biochem. J.* **320**, 61–67
- Gralla, E. B., and Valentine, J. S. (1991) *J. Bacteriol.* **173**, 5918–5920
- van Loon, A. P., Pesold-Hurt, B., and Schatz, G. (1986) *Proc. Natl. Acad. Sci. U. S. A.* **83**, 3820–3824
- Ahn, S. M., Lee, S. M., Chung, T., Kim, K., and Park, J. W. (1996) *Biochem. Mol. Biol. Int.* **39**, 1007–1015
- Chae, H. Z., and Rhee, S. G. (1994) *Biofactors* **4**, 177–180
- Chae, H. Z., Chung, S. J., and Rhee, S. G. (1994) *J. Biol. Chem.* **269**, 27670–27678
- Grant, C. M., Collinson, L. P., Roe, J. H., and Dawes, I. W. (1996) *Mol. Microbiol.* **21**, 171–179
- Kuge, S., and Jones, N. (1994) *EMBO J.* **13**, 655–664
- Garrard, L. J., and Goodman, J. M. (1989) *J. Biol. Chem.* **264**, 13929–13937
- Gan, Z. R. (1992) *Biochem. Biophys. Res. Commun.* **187**, 949–955
- Babychuck, E., Kushnir, S., Belles-Boix, E., Van Montagu, M., and Inzé, D. (1995) *J. Biol. Chem.* **270**, 26224–26231
- Srivastava, S., Chandra, A., Bhatnagar, A., Srivastava, S. K., and Ansari, N. H. (1995) *Biochem. Biophys. Res. Commun.* **217**, 741–746
- Spycher, S. E., Tabataba-Vakili, S., O'Donnell, V. B., Palomba, L., and Azzi, A. (1997) *FASEB J.* **11**, 181–188
- Mager, W. H., and Moradas Ferreira, P. (1993) *Biochem. J.* **290**, 1–13
- Mager, W. H., and De Kruuff, A. J. J. (1995) *Microbiol. Rev.* **59**, 506–531
- Shang, F., Gong, X., and Taylor, A. (1997) *J. Biol. Chem.* **272**, 23086–23093
- Grune, T., Reinheckel, T., and Davies, K. J. (1996) *J. Biol. Chem.* **271**, 15504–15509
- Hilt, W., and Wolf, D. (1996) *Trends Biochem. Sci.* **21**, 96–102
- Ciechanover, A., Laszlo, A., Bercovich, B., Stancovski, I., Alkalay, I., Ben-Neriah, Y., and Orian, A. (1995) *Cold Spring Harbor Symp. Quant. Biol.* **60**, 491–501
- Ribeiro, M. J., Silva, J. T., and Panek, A. D. (1994) *Biochim. Biophys. Acta* **1200**, 139–147
- De Virgilio, C., Hottiger, T., Dominguez, J., Boller, T., and Wiemken, A. (1994) *Eur. J. Biochem.* **219**, 179–186
- Gounalaki, N., and Thireos, G. (1994) *EMBO J.* **13**, 4036–4041
- Wiemken, A. (1990) *Antonie van Leeuwenhoek* **58**, 209–217
- Parrou, J.-L., Teste, M.-A., and Francois, J. (1997) *Microbiology* **143**, 1891–1900
- Zahringer, H., Burgert, M., Holzer, H., and Nwaka, S. (1997) *FEBS Lett.* **412**, 615–620
- Schaaff-Gerstenschlager, I., and Zimmermann, F. K. (1993) *Curr. Genet.* **24**, 373–376

49. Berthon, H. A., Kuchel, P. W., and Nixon, P. F. (1992) *Biochemistry* **31**, 12792–12798
50. Norbeck, J., and Blomberg, A. (1997) *J. Biol. Chem.* **272**, 5544–5554
51. Noga, I., and Johnston, M. (1990) *Gene (Amst.)* **96**, 161–169
52. Muller, E. G. (1996) *Mol. Biol. Cell* **7**, 1805–1813
53. Juhnke, H., Krems, B., Kotter, P., and Entian, K.-D. (1996) *Mol. Gen. Genet.* **252**, 456–464
54. Hudak Slekar, K., Kosman, D. J., and Culotta, V. C. (1996) *J. Biol. Chem.* **271**, 28831–28836
55. Thomas, D., Cherest, H., and Surdin-Kerjan, Y. (1991) *EMBO J.* **10**, 547–553
56. Velculescu, V. E., Zhang, L., Zhou, W., Vogelstein, J., Basrai, M. A., Bassett Jr, D. E., Hieter, P., Vogelstein, B., and Kinzler, K. W. (1997) *Cell* **88**, 243–251
57. DeRisi, J. L., Lyer, V. R., and Brown, P. O. (1997) *Science* **278**, 680–686
58. Krems, B., Charizanis, C., and Entian, K.-D. (1995) *Curr. Genet.* **27**, 427–434
59. Krems, B., Charizanis, C., and Entian, K.-D. (1996) *Curr. Genet.* **29**, 327–334
60. Morgan, B. A., Banks, G. R., Toone, W. M., Raitt, D., Kuge, S., and Johnston, L. H. (1997) *EMBO J.* **16**, 101–110
61. Martinez-Pastor, M. T., Marchler, G., Schüller, C., Marchler-Bauer, A., Ruis, H., and Estruch, F. (1996) *EMBO J.* **15**, 227–2235
62. Liu, X.-D., and Thiele, D. J. (1996) *Genes Dev.* **10**, 592–603
63. Engelberg, D., Klein, C., Martinetto, H., Struhl, K., and Karin, M. (1994) *Cell* **77**, 381–390